THE EFFECT OF COMPRESSIBILITY ON THE KELVIN-HELMHOLTZ INSTABILITY IN PLASMAS

A. G. González[1-3], J. Gratton[2-3*]

1 Instituto de Física Arroyo Seco-Univ. Nac. del Centro de la Pcia. de Buenos Aires, Pinto 399, Tandil
2 INFIP-CONICET, Fac. de Cs. Exactas y Naturales-Univ. de Buenos Aires, C. Universitaria, Pab. I, Bs. As.
3 Investigador del CONICET
e-mail: jgratton@tinfip.lfp.uba.ar

La inestabilidad de Kelvin-Helmholtz se presenta en muchos plasmas naturales y de laboratorio, en configuraciones muchas veces complejas con cizalla magnética y diferencias de densidad y temperatura de ambos lados de la discontinuidad de velocidad. La inclusión de los efectos de la compresibilidad lleva a notables complicaciones debido a que la relación de dispersión lleva en general a un polinomio de grado 10 que depende de 6 parámetros independientes. Por este motivo en la interpretación de los datos experimentales se suele usar el resultado de la teoría incompresible ya que en esa aproximación la condición de estabilidad se expresa en forma analítica, y además porque en base a los conocidos teoremas de Newcomb, se piensa que la compresibilidad tiende a estabilizar los modos de Kelvin-Helmholtz. Sin embargo dichos teoremas no se pueden aplicar en esta caso dado que al haber movimiento de masa es posible tener perturbaciones de energía negativa, y por lo tanto se puede generar una nueva inestabilidad si debido a la compresibilidad aparecen nuevos modos. En este trabajo mostramos que efectivamente, el efecto de la compresibilidad lleva a desestabilizar el plasma para bajas velocidades relativas en situaciones que son estables en el límite incompresible.

The Kelvin-Helmholtz instability occurs in many natural and laboratory plasmas, in complex configurations with magnetic shear and density and temperature jumps across the velocity. The addition of compressibility effects leads to notable complexities since the dispersion relation yields a polynomial of tenth degree that depends on 6 independent parameters. Then, the results of the incompressible theory are usually employed while interpreting experimental data since in this approximation the stability condition has an analytical form, and it is assumed that compressibility tends to stabilize the Kelvin-Helmholtz modes, an assumption based on the Newcomb's well-known theorems. Nevertheless these theorems cannot be applied in our case because perturbations with negative energy are possible in configurations with mass flow, and in consequence new instabilities may develop if new modes appear due to compressibility. In this paper we show that the effect of compressibility destabilizes the plasma for low relative velocities in cases that were stable in the incompressible limit.

I. INTRODUCTION

The Kelvin-Helmholtz Instability (KHI) occurs in many laboratory and astrophysical plasmas, usually in complex configurations in which the properties of the plasma change across a transition layer separating two uniform regions in relative. In many circumstances, the problem can be modeled using a plane slab geometry, in which the unperturbed quantities (density ρ, pressure p, magnetic field $\boldsymbol{B}$ and mass flow velocity $\boldsymbol{u}$) depend only on the y coordinate (perpendicular to the transition layer). A differential equation for the linear MHD perturbations of stratified plasmas[1] can be used as a starting point to investigate these problems. If the wavelength of the perturbation is large as compared to the thickness of the transition layer, we can ignore the structure inside the transition and consider the latter as a surface (at y=0) separating two infinite, uniform plasma regions. The problem can then be treated by means of standard normal mode analysis. The equations of ideal MHD and the parameters of the configuration do not involve either a frequency or a length scale. Therefore the (complex) phase velocity v of the perturbation ($v \equiv \omega / k_t$) is a function of the parameters of the plasma, of the mass velocities of the uniform regions and of the wavenumber $\mathbf{k}_t \equiv (k_x, 0, k_z)$ of the perturbation and an algebraic dispersion relation is obtained.

The incompressible MHD approximation (IMHD) is often employed in space physics to interpret the observed data and to examine the stability of the configuration. The tacit assumption is that compressibility effects thus neglected should (if any) improve stability. This assumption is based on well-known theorems[2] according to which the introduction of compressibility leads to a positive contribution to the energy of the plasma and so tends to stabilize it. However, these results cannot be applied in our case, since owing to the presence of mass flow the plasma can sustain perturbations with a *negative* energy density that can lead to instability[3,4]. A negative energy density perturbation may lead to instability if it couples to a positive energy density perturbation, since then both can grow without an external source of energy. In IMHD, the instability arises from perturbations of the interface that are exponentially damped in both plasma regions. The instability occurs when u_k exceeds a critical value u_t, such that their energy density (in the laboratory frame) is

[*] Autor a quién debe dirigirse la correspondencia.

positive in one region and negative in the other. It grows because energy is transferred across the interface from the negative energy density region to the other, and remains localized, as it cannot be transported across the magnetic field. We call it *primary* KHI.

In the compressible MHD (CMHD) there are fast and slow magnetosonic waves that propagate in the bulk of the plasma and transport energy *across* the magnetic field. Consequently, the effect of compressibility on the MHD Kelvin-Helmholtz instability is complex, leading to the stabilization of certain perturbations and to the *destabilization* of others.

Consider first the primary KHI. Due to compressibility, if u_k is sufficiently large the perturbation may be able to propagate in both regions as fast magnetosonic waves. When this happens, the observer sees a pair of fast magnetosonic waves radiated away from the interface. One of these waves has a negative, and the other a positive energy density[3,4]. In this way, perturbations that are unstable according to IMHD are *stabilized* by compressibility. However, in addition to this large-u_k stabilization, there is a *destabilizing* effect of compressibility, namely that the critical value u_c for the onset of the instability is *lowered* ($u_c \leq u_i$). Stable perturbations according to IMHD become unstable when compressibility is taken into account.

Due to the presence of slow magnetosonic waves *new kinds* of perturbations of the interface are possible, which have no counterpart in IMHD. Some of them are stable evanescent oscillations, or may consist of slow magnetosonic waves in both regions (radiation of a pair of slow magnetosonic waves), but some are *unstable*. These new instabilities (called *secondary* KHI) are found in intervals of u_k that correspond to stable perturbations according to IMHD, and are totally, or partially, *below* the critical u_k value for the onset of the primary KHI. The occurrence of the secondary KHI is an additional *destabilizing* effect of compressibility. The growth rates of the secondary modes are usually small. However these modes cannot be ignored, since in some configurations of interest for magnetopause applications they are the only unstable modes present.

II. COMPRESSIBLE PERTURBATIONS

Our treatment[5] includes arbitrary jumps in the velocity, magnetic fields, density and temperature, without restriction on the direction of the wave vector of the perturbation. The configuration consists of two uniform plasma regions in relative motion with constant velocity $\mathbf{u}'_1$ in region 1 ($y>0$), and $\mathbf{u}'_2$ in region 2 ($y<0$). The flow velocities $\mathbf{u}'_1$ and $\mathbf{u}'_2$ and the magnetic fields $\boldsymbol{B}_1$ and $\boldsymbol{B}_2$ are parallel to the plane $y=0$, the suffixes $i=1,2$ denote quantities pertaining to region 1 and 2, respectively. At the interface $y=0$ the pressure (p), the density (ρ) and the magnetic field can have arbitrary discontinuities, subject to the equilibrium condition.

We shall assume ideal CMHD and consider linear adiabatic perturbations of the unperturbed configuration. Since the growth rate of the instability does not depend on $\mathbf{u}'_1$ and $\mathbf{u}'_2$ separately, but only on their difference $2\mathbf{u}=\mathbf{u}'_1-\mathbf{u}'_2$, it is convenient to use a reference frame moving with $\mathbf{u}'=(\mathbf{u}'_1+\mathbf{u}'_2)/2$, where $\mathbf{u}_1=\mathbf{u}=u\mathbf{e}_x$, $\mathbf{u}_2=-\mathbf{u}$. The wavenumber of the perturbation of the interface is $\mathbf{k}_t \equiv (k_x, 0, k_z)$ and ω is its frequency in the average velocity frame; the phase velocity is then $v=\omega/k_t$. The Doppler-shifted frequencies in the plasma frames are then $\omega_1=\omega-u_k k_t$ in region 1 and $\omega_2=\omega+u_k k_t$ in region 2, and the corresponding phase velocities are $v_i=\omega_i/k_t$, i. e. $v_1=v-u_k$ and $v_2=v+u_k$. We shall denote by ψ_i the angles between $\boldsymbol{B}_i$ and $\boldsymbol{k}_t$, and by φ_i the angles between $\boldsymbol{B}_i$ and $\boldsymbol{u}$. The angle between $\boldsymbol{k}_t$ and $\boldsymbol{u}$ is α, so that $u_k=u\cos\alpha$. The Alfvén and sound velocity are respectively

$$A_i \equiv B_i/\sqrt{4\pi\rho_i}\,,\quad S_i \equiv \sqrt{\gamma p_i/\rho_i}\ (\gamma=5/3) \qquad (1)$$

and we shall use the following definitions

$$d_i=\sqrt{A_i^2+S_i^2}\,,\ a_i=A_i\cos\psi_i\,,\ b_i=a_i S_i/d_i \qquad (2)$$

$$p_i, m_i=\sqrt{\tfrac{1}{2}\left(d_i^2 \pm \sqrt{d_i^4-4d_i^2 b_i^2}\right)} \qquad (3)$$

$$\Gamma_i=\sqrt{-\frac{(v_i^2-p_i^2)(v_i^2-m_i^2)}{d_i^2(v_i^2-b_i^2)}} \qquad (4)$$

(with $\mathrm{Re}(\Gamma_i)>0$, or $\mathrm{Im}(\Gamma_i)>0$ if $\mathrm{Re}(\Gamma_i)=0$). In each region, the general form of the perturbation is

$$\zeta_i=e^{i(\mathbf{k}_t\cdot\mathbf{x}-\omega t)}\left(C_i e^{-k_t\Gamma_i y}+D_i e^{k_t\Gamma_i y}\right) \qquad (5)$$

In Eq. (5), ζ_i is the y-component of the displacement, and C_i and D_i are constants. The penetration depth of the perturbation in region i is proportional to $1/\mathrm{Re}(\Gamma_i)$. When $\mathrm{Re}(\Gamma_i)=0$, Eq. (4) corresponds to fast and slow magnetosonic waves in a semi-infinite uniform moving plasma; whose wave vector is $(k_x, k_t\,\mathrm{Im}(\Gamma_i), k_z)$. When $\mathrm{Re}(\Gamma_i)\neq 0$, Eq (4) corresponds to evanescent perturbations and of course in this case the amplitudes of the exponentially growing perturbations (D_1 and C_2) must vanish since the plasma extends to ± infinity.

The continuity of the displacement and of the normal stress at the interface couple the perturbations of regions 1 and 2 and leads to a matrix equation:

$$\begin{bmatrix} C_1 \\ D_1 \end{bmatrix}=\frac{\Gamma_1}{2\rho_1(v_1^2-a_1^2)}\begin{bmatrix} T & S \\ S & T \end{bmatrix}\begin{bmatrix} C_2 \\ D_2 \end{bmatrix}, \qquad (6)$$

$$T=\frac{\rho_1(v_1^2-a_1^2)}{\Gamma_1}-\frac{\rho_2(v_2^2-a_2^2)}{\Gamma_2}\,, \qquad (7)$$

$$S=\frac{\rho_1(v_1^2-a_1^2)}{\Gamma_1}+\frac{\rho_2(v_2^2-a_2^2)}{\Gamma_2}\,. \qquad (8)$$

The matrix equation may be used to investigate problems involving localized modes as well as the reflection and transmission of magnetosonic waves. The unstable modes and the stable surface oscillations have

$\mathrm{Re}(\Gamma_{1,2}) \neq 0$. In this case we must have $C_1 = D_2 = 0$. Therefore the corresponding dispersion relation is

$$T = 0 \qquad (9)$$

The propagating modes have $\mathrm{Re}(\Gamma_{1,2}) = 0$, and there is no restriction on C_i, D_i. In this case, $T = 0$ and $S = 0$ determine the poles and zeros of the reflection coefficient. Since the sign of the y-component of the group velocity of magnetosonic waves may be different from the sign of $\mathrm{Re}(\Gamma_{1,2})$, one must examine the group velocities in each region, to ascertain which of these conditions yields the dispersion relation for *radiation* of a pair of waves, or for *total transmission* of waves.

To investigate the roots of (9) it is useful to introduce a polynomial P that is obtained by taking the numerator of the product TS, thus eliminating the square roots. Clearly, the roots of $P = 0$ encompass the solutions of $T = 0$ as well as those of $S = 0$, and we must discard the latter when we look for localized modes. We call 'true branch' (T) the set of solutions of $T = 0$ and 'spurious branch' (S) the solutions of $S = 0$. The T-branch and the S-branch consist of several continuous manifolds in the parameter space of the problem. If the parameters change, a root v (real or complex) of P that belongs to a certain segment T_j moves along it,, until eventually it arrives to the boundary and ceases to belong to the true branch and becomes spurious. Note that the T-S boundaries occur only for *real* values of v, at the points where $\Gamma_{1,2}$=0,∞. A convenient way to visualize the *real* roots of the dispersion relation and to unravel the topology of the T and S branches is to use a graphical method first employed by Chandrasekhar[6]. It uses the fact that finding the roots v of $P = 0$ is equivalent to solving for v_1 and v_2 the coupled equations:

$$P(v_1, v_2) = 0, \quad v_2 = v_1 + 2u_k \qquad (10)$$

Their *real* solutions can be found in a (v_1, v_2) diagram as the intersections of the line L given by (10b) with the curves $v_2 = v_2(v_1)$ that are obtained solving the bi-cubic (in v_1 and v_2) equation (10a) for v_2. It suffices to consider only a quadrant, since the curves $v_2 = v_2(v_1)$ are symmetrical under reflections on both axes. In this diagram the lines $v_2 = v_1$ and $v_2 = -v_1$ represent the v- and u_k- axes (except from a scale factor √2). A real root belongs to the T branch if $\mathrm{Sign}(v_1^2 - a_1^2) \neq \mathrm{Sign}(v_2^2 - a_2^2)$ (i. e., if $|v_1| < a_1$ and $|v_2| > a_2$, or $|v_1| > a_1$ and $|v_2| < a_2$); if otherwise, it belongs to the S-branch. Both branches must be considered for radiation and total transmission modes.

For certain u_k, L is tangent to the curves and the roots coalesce. This might correspond to marginal stability. An analysis of the diagrams shows that there can be up to *six* positive values of u_k corresponding to significant (i.e., belonging to the T-branch) double roots of $P(v) = 0$ $(u_{d1}, \ldots, u_{d6})$ and there can be up to three unstable intervals: (a) $u_{d1} < u_k < u_{d3}$ that we shall call secondary interval A, (b) $u_{d2} < u_k < u_{d4}$ or secondary interval B and (c) $u_{d5} < u_k < u_{d6}$ or primary interval. As the parameters are varied, it may happen that the pair u_{d3} and u_{d5}, or the pair u_{d4} and u_{d5}, coalesce and become complex. In the first case, the secondary interval A merges with the Primary interval. In the second case, the secondary interval B is merged with the principal interval. Notice that the secondary intervals can partially or totally overlap. These intervals can be extremely narrow for some values of the parameters, and they vanish for flute perturbations in either region 1 or 2. For negative u_k, a completely symmetrical result is obtained, in which the signs of the inequalities are reversed.

III. THE SECONDARY KELVIN-HELMHOLTZ INSTABILITY

In the incompressible limit ($S_1, S_2 \to \infty$) the secondary unstable intervals disappear, and we are left only with a main unstable interval that extends to infinity. Then, the secondary KHI and the large u_k stabilization of the primary KHI at u_{d6} are consequences of compressibility. To see the origin of the secondary KHI, we note that $P(v_1, v_2)$ can be written as:

$$P(v_1, v_2) = S_1^2 S_2^2 P_{inc} + S_1^2 P_1 + S_2^2 P_2 + P_3 \qquad (11)$$

$P_{inc} = (v_1^2 - a_1^2)(v_2^2 - a_2^2)[\rho_1^2 (v_1^2 - a_1^2)^2 - \rho_2^2 (v_2^2 - a_2^2)^2]$ and P_1, P_2, P_3, are polynomials whose coefficients are functions of a_1, a_2, A_1, A_2, ρ_1 and ρ_2. In the limit $S_1, S_2 \to \infty$, if we assume that $v_{1,2}$ remain finite, the equation (11) reduces to $P_{inc} = 0$. Solving it, one finds two roots that are stable, and correspond to Alfvén waves propagating in regions 1 and 2, respectively: $v = v_{a1\pm} \equiv u_k \pm a_1$, $v = v_{a2\pm} \equiv -u_k \pm a_2$. The roots[6]:

$$v = v_{K\pm} \equiv u_k \frac{\rho_1 - \rho_2}{\rho_1 + \rho_2} \pm \sqrt{\frac{(a_1^2 \rho_1 + a_2^2 \rho_2)}{\rho_1 + \rho_2} - \frac{4u_k^2 \rho_1 \rho_2}{(\rho_1 + \rho_2)^2}}$$

yield the incompressible Kelvin-Helmholtz instability for

$$|u_k| > u_i = \frac{1}{2}\sqrt{\frac{\rho_1 + \rho_2}{\rho_1 \rho_2}(a_1^2 \rho_1 + a_2^2 \rho_2)} \qquad (12)$$

Finally, the roots

$$v = v_{S\pm} \equiv u_k \frac{\rho_1 + \rho_2}{\rho_1 - \rho_2} \pm \sqrt{\frac{(a_1^2 \rho_1 - a_2^2 \rho_2)}{\rho_1 - \rho_2} - \frac{4u_k^2 \rho_1 \rho_2}{(\rho_1 - \rho_2)^2}}$$

are spurious. Some of these roots can coincide for certain u_k. For example, when $u_k = u_D \equiv (a_1 + a_2)/2$ the roots v_{a1-}, v_{a2+}, $v_{K\pm}$, (± according to the sign of $a_1^2 \rho_1 - a_2^2 \rho_2$) and v_{S-} coincide and their value is $v = v_D \equiv (-a_1 + a_2)/2$. This degeneracy corresponds to $v_1 = -a_1$ and $v_2 = -a_2$. It can be verified that $u_i \geq u_D$. Now, let us assume that S_1,S_2 are large, but finite. Then the terms $S_1^2 P_1(v_1, v_2) + S_2^2 P_2(v_1, v_2)$ in (11) can be treated as a small perturbation that couples the degenerate roots v_{a1-}, v_{a2-}, $v_{K\pm}$, and v_{S-}. It can be shown that part of the degeneracy is removed, and some roots acquire an imaginary part. The unstable modes that appear in this way (Secondary KHI) have no analogue among the purely incompressible modes. This instability appears around $u_k \approx u_D$, that is, in a range of u_k that is stable according to IMHD, since it lies below u_i. There are three other points where degeneracy of the roots occurs. The removal of the degeneracy due to compressibility at $u = -u_D, v = -v_D$ leads to overstable modes like in the case described above, but not at other points.

IV. STABILITY DIAGRAMS

The problem of finding the localized eigenmodes requires solving the ten-degree polynomial P. In addition, the problem involves *seven* independent parameters. Five of them characterize the plasma configuration; they can be taken as $r_b = B_2 / B_1$, $r_s = S_2 / S_1$ and $r_d = \rho_2 / \rho_1$, the relative velocity u, and the angles φ_1 from $\boldsymbol{B}_1$ to $\boldsymbol{u}$ and θ from $\boldsymbol{B}_1$ to $\boldsymbol{B}_2$ (magnetic shear angle). The remaining is the angle ψ_1 from $\boldsymbol{B}_1$ to $\boldsymbol{k}_t$, which identifies the perturbation we are considering. Note that P (and its roots) depends on u only through the combination

$$u_k \equiv u \cos\alpha = u \cos(\psi_1 - \varphi_1) \qquad (13)$$

We shall represent the results using diagrams in which we plot the growth rate $\mathrm{Im}(v)$ of the unstable modes as functions of ψ_1 and u_k, keeping fixed the remaining parameters. An example is shown in Fig. 1, where we have drawn a contour plot of $\mathrm{Im}(v)$ for parameters from spacecraft data taken on January 11, 1997 in a region near a flank of the mangetopause (r_b=1.5, r_s=2.67, r_d=0.117, $\theta = -80°$). Notice that this plot does not refer to a particular plasma configuration (since we have not yet specified u and φ_1): it can be used for any configuration with the same r_b, r_s, r_d and θ. If at the same point (ψ_1, u_k) there are *two* unstable roots, we only represent the larger of the two values of $\mathrm{Im}(v)$.

In Fig. 1, we have also drawn the curve $u_i(\psi_1)$ given by eq. (12). All the points of the stability diagram above $u_i(\psi_1)$ correspond to instability according to IMHD. Several effects of compressibility are easily recognized: (a) a large-u_k stabilization of the Primary instability, (b) a small-u_k destabilization of the Primary instability and (d) a presence of the Secondary instability for values of u_k that are stable according to IMHD. It should also be mentioned that for $u_k > u_i(\psi_1)$ (but not very close to it) the growth rates calculated with CMHD are always smaller than those calculated with IMHD.

To investigate a particular configuration by means of the stability diagram we must draw the curve C given by eq. (13). Following C we find the value of $\mathrm{Im}(v)$ for the configuration, for any perturbation characterized by the angle ψ_1. Since the problem is invariant under the transformation ($v \to -v$, $u_k \to -u_k$), it suffices to calculate the contour plot for $u_k \geq 0$ and then draw the curve C' given by $u_k = -u\cos\alpha$ in addition to C. In our example the configuration described by the curves C and C' ($u = 1.7A_1$, $\varphi_1 = -89.9°$) is *stable* according to IMHD, but it is *unstable* if compressibility is taken into account. The unstable modes occur in the range $40° \leq \psi_1 \leq 50°$ and they belong to the secondary KHI. Their maximum growth rate is small ($\mathrm{Im}(v) \approx 0.04A_1$), but significant. Other configurations with the same values of r_b, r_s, r_d and θ can be more unstable. The extreme of $\mathrm{Im}(v)$ is $\approx 2.115A_1$; it occurs for $\psi_1 \approx 25°$ and $u_k \approx 5A_1$.

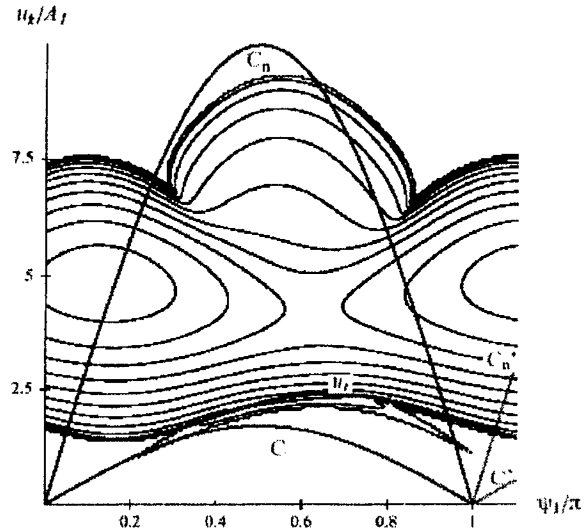

Fig. 1. Stability diagram. The contours of $\mathrm{Im}(v)$ *are spaced by* $0.2A_1$.

In order to clarify the meaning of the large-u_k stabilization, let us consider a configuration with $u = 10A_1$ and $\varphi_1 = -90°$. The new curves C_n and C_n' will be similar to C and C'. Part of C_n (for $45° < \psi_1 < 113°$) will lie in the upper part of the stability diagram ($u_k > u_{d6}$) corresponding to stable perturbations: these are the large-u_k stabilized modes. However, this configuration is unstable, since C_n and C_n' must necessarily pass through the unstable part of the diagram. Actually, the most unstable modes have $\mathrm{Im}(v)$ very close to the extreme value for the diagram.

This work was supported by grants of the University of Buenos Aires (Project TW16) and of CONICET (PIP4521).

References

1 - Gratton, F., Gratton, J., and González, A.G. Plasma Phys. & Controlled Fusion **30**, 435-456 (1988).

2 - Newcomb, W.A. Phys. Fluids **26**, 3246 (1983).

3 - Kivelson, M.G., Pu, Z.Y. Planet. Space Sci. **32**. 1335 (1984).

4 - González, A.G. and Gratton, J. in Proc. VIII Latin-American Workshop on Plasma Physics. Vol. 1, p. 23-54. Tandil (1998).

5 - González, A.G. and Gratton, J. J. Plasma Phys. **52**, 233-244 (1994).

6 - Chandrasekhar, S. Hydrodynamic and Hydromagnetic Stability, Oxford Univ. Press (1961)